Geophysical Research Letters

RESEARCH LETTER
10.1029/2021GL093805

Special Section:
Fire in the Earth System

# Measuring Atmospheric $CO_2$ Enhancements From the 2017 British Columbia Wildfires Using a Lidar

**Jianping Mao[1,2], James B. Abshire[1,2], Stephan R. Kawa[2], Haris Riris[2], Xiaoli Sun[2], Niels Andela[3], and Paul T. Kolbeck[1]**

[1]University of Maryland, College Park, MD, USA, [2]NASA Goddard Space Flight Center, Greenbelt, MD, USA, [3]Cardiff University, Cardiff, UK

**Key Points:**

- NASA Goddard $CO_2$ Sounder Lidar can accurately measure $CO_2$ enhancements from wildfires through dense smoke plumes
- This is the first use of lidar to remotely sense $CO_2$ enhancements from large wildfires
- These types of lidar measurements can be used to validate estimates of $CO_2$ emissions from wildfires and improve estimates of carbon fluxes

**Correspondence to:**
J. Mao,
jianping.mao@nasa.gov

**Citation:**
Mao, J., Abshire, J. B., Kawa, S. R., Riris, H., Sun, X., Andela, N., & Kolbeck, P. T. (2021). Measuring atmospheric $CO_2$ enhancements from the 2017 British Columbia wildfires using a lidar. *Geophysical Research Letters*, *48*, e2021GL093805. https://doi.org/10.1029/2021GL093805

Received 9 APR 2021
Accepted 3 AUG 2021



**Abstract** During the summer 2017 ASCENDS/ABoVE airborne science campaign, the NASA Goddard $CO_2$ Sounder lidar overflew smoke plumes from wildfires in the British Columbia, Canada. In the flight path over Vancouver Island on 8 August 2017, the column $XCO_2$ retrievals from the lidar measurements at flight altitudes around 9 km showed an average enhancement of 4 ppm from the wildfires. A comparison of these enhancements with those from the Goddard Global Chemistry Transport model suggested that the modeled $CO_2$ emissions from wildfires were underestimated by more than a factor of 2. A spiral-down validation performed at Moses Lake airport, Washington showed a bias of 0.1 ppm relative to in situ measurements and a standard deviation of 1 ppm in lidar $XCO_2$ retrievals. The results show that future airborne campaigns and spaceborne missions with this type of lidar can improve estimates of $CO_2$ emissions from wildfires and estimates of carbon fluxes globally.

**Plain Language Summary** Wildfires are a major source of greenhouse gases. However, there are large uncertainties in the estimated $CO_2$ emissions from wildfires in global emissions inventories. The estimates of column-averaged $CO_2$ ($XCO_2$) from satellite measurements using passive remote sensing techniques are significantly degraded or screened out by the scattering from smoke in the scene. NASA Goddard Space Flight Center has developed an integrated-path, differential absorption lidar approach to measure $XCO_2$ from space. Measurements of time-resolved laser backscatter profiles from the atmosphere allow this technique to accurately estimate $XCO_2$ and range to terrain and water surfaces even in the presence of wildfire smoke. We demonstrate this capability over Vancouver Island through the dense smoke plumes from wildfires in the Canadian Rockies during the summer 2017 ASCENDS/ABoVE airborne science campaign. To our knowledge this is the first use of lidar to remotely sense $CO_2$ enhancements from large wildfires. Future airborne campaigns and spaceborne missions with this capability can improve estimates of $CO_2$ emissions from wildfires and help estimates of carbon fluxes globally.

## 1. Introduction

Wildfires are a major source of greenhouse gases. Fires were responsible for as much as a fifth of the carbon released in 2019 from burning fossil fuels, down from about a quarter at the beginning of the century (Ciais et al., 2013; Le Quéré et al., 2018; Tian et al., 2016). While this long-term decrease in fire emissions was driven by a decline in savanna and grassland fires (Andela et al., 2017), a recent increase in forest fires has resulted in concerns about the future role of fire in the global carbon cycle. Total carbon emissions from forest fires in 2019 were 26% higher than in 2018, to 7.8 billion metric tons, the highest since 2002, according to the Global Fire Emissions Database (GFED; van der Werf et al., 2017). The unprecedented bushfires in Australia in 2019 emitted a combined 306 million metric tons of carbon dioxide ($CO_2$) in the August–December 2019 period, which is more than half of Australia's total carbon footprint in the year. Brazilian Amazon fires emitted 392 million metric tons of $CO_2$ in 2019 which was equivalent to more than 80% of Brazil's 2018 greenhouse gas emissions (Lombrana et al., 2020).

During 2017, Canada had a record-breaking wildfire season in the province of British Columbia (BC). A total of 1.2 million hectares had burned by the end of the 2017 fire season, the largest ever in the province (Duran, 2017) and massive smoke plumes were lofted into the stratosphere in the mid-August (Torres et al., 2020).

Generally, there are large uncertainties in the estimated $CO_2$ emissions from wildfires with fire emissions inventories (Andreae, 2019; Meyer et al., 2012). Ground-based and airborne measurements of fire emissions are few and are difficult to obtain. Atmospheric column-averaged dry air mole fraction of $CO_2$ ($XCO_2$) retrievals using surface reflected sunlight, for example, the Orbiting Carbon Observatory-2 (OCO-2; Crisp et al., 2004) and the Greenhouse gases Observation SATellite (GOSAT; Kuze et al., 2016) are significantly degraded by scattering effects of fire smoke in the scene (Aben et al., 2007; Butz et al., 2009; Guerlet et al., 2013; Houweling et al., 2005; Mao & Kawa, 2004; Uchino et al., 2012).

NASA Goddard Space Flight Center has developed an integrated-path, differential absorption (IPDA) lidar approach to measure global $XCO_2$ from space as a candidate for NASA's planned Active Sensing of $CO_2$ Emissions over Nights, Days, and Seasons (ASCENDS) mission (Kawa et al., 2018). This pulsed laser approach uses a step-locked laser source and a high-efficiency detector to measure atmospheric absorption at multiple wavelengths across the $CO_2$ line centered at 1572.335 nm. It has a high spectral resolution and sub-ppm sensitivity to changes in $XCO_2$ (Abshire et al., 2018). Measurements of time-resolved atmospheric backscatter profiles allow this technique to estimate $XCO_2$ and range to any significant reflective surfaces with precise knowledge of the photon path-length even in the presence of atmospheric scattering (Mao et al., 2018; Ramanathan et al., 2015).

During July and August 2017, NASA conducted a joint ASCENDS/ABoVE (Arctic Boreal Vulnerability Experiment) airborne science campaign using the NASA DC-8 aircraft based in Fairbanks, Alaska (Mao et al., 2019). The $CO_2$ Sounder lidar measured $XCO_2$ from aircraft altitudes to ground, along with height-resolved backscatter profiles. Other instruments on the DC-8 aircraft included the NASA Langley Research Center ACES $CO_2$ lidar (Obland et al., 2018) along with a suite of in situ instruments including AVOCET for $CO_2$ (Halliday et al., 2019), Picarro for $CO_2$, $CH_4$, and $H_2O$, and an engineering test version of DLH for $H_2O$, CO, $CH_4$, and $N_2O$ (Diskin et al., 2002). The DC-8 aircraft's housekeeping data provided temperature, pressure, geolocation, and positioning such as altitude and pitch/roll angles at flight altitude. Its radar altimeter also provides a reference for ground elevation under all conditions since the radar measurement penetrates clouds and smoke.

During the return flight from Alaska to California on August 8, the aircraft overflew dense smoke plumes from fires in the Canadian Rockies on the segment from Vancouver Island to central Washington State. Here we present the $XCO_2$ and backscatter measurements over this region along with the validation spiral maneuver at Moses Lake airport in central Washington, performed shortly after the region of $XCO_2$ enhancement. We then compare the measured $XCO_2$ enhancements with those from the Goddard Parameterized Chemistry Transport Model (PCTM) using GFED. This case study demonstrates the capability of the $CO_2$ Sounder lidar approach to measure enhanced $XCO_2$ through dense smoke plumes, which allows improving the estimates of $CO_2$ emissions from wildfires.

## 2. Lidar Measurements From 2017 ASCENDS/ABoVE Airborne Science Campaign

### 2.1. 2017 ASCENDS/ABoVE Airborne Campaign to Alaska

The $CO_2$ Sounder lidar has flown on DC-8 five times since 2010 over a variety of sites in the US, along with other ASCENDS airborne lidar candidates and in situ $CO_2$ sensors (Abshire et al., 2010, 2013, 2014, 2018). The ASCENDS/ABoVE airborne science campaign to Alaska was the first to extend these lidar measurement to the arctic region. The 2017 campaign also allowed determining the horizontal gradients in $XCO_2$ during the long transit flights between California and Alaska. In all, eight flights were conducted over the Central Valley of California, the Northwest Territory Canada, and south and central Alaska between July 20 and August 8, 2017. Forty-seven vertical spiral maneuvers were conducted over a variety of atmospheres and surface types like desert, vegetation, permafrost, and both the Pacific and Arctic Oceans. The $XCO_2$ retrievals from the lidar measurements were validated against those computed from in situ measurements of $CO_2$ vertical profiles made during the spiral maneuvers.

The final flight of the campaign was conducted on August 8, 2017, based out of Fairbanks, AK and transited south back to Palmdale, CA (Figure 1, top panel). The flight had six spiral-down maneuvers when over land including ones at Northway airport in Alaska, Whitehorse airport in Yukon, Canada, Moses Lake airport

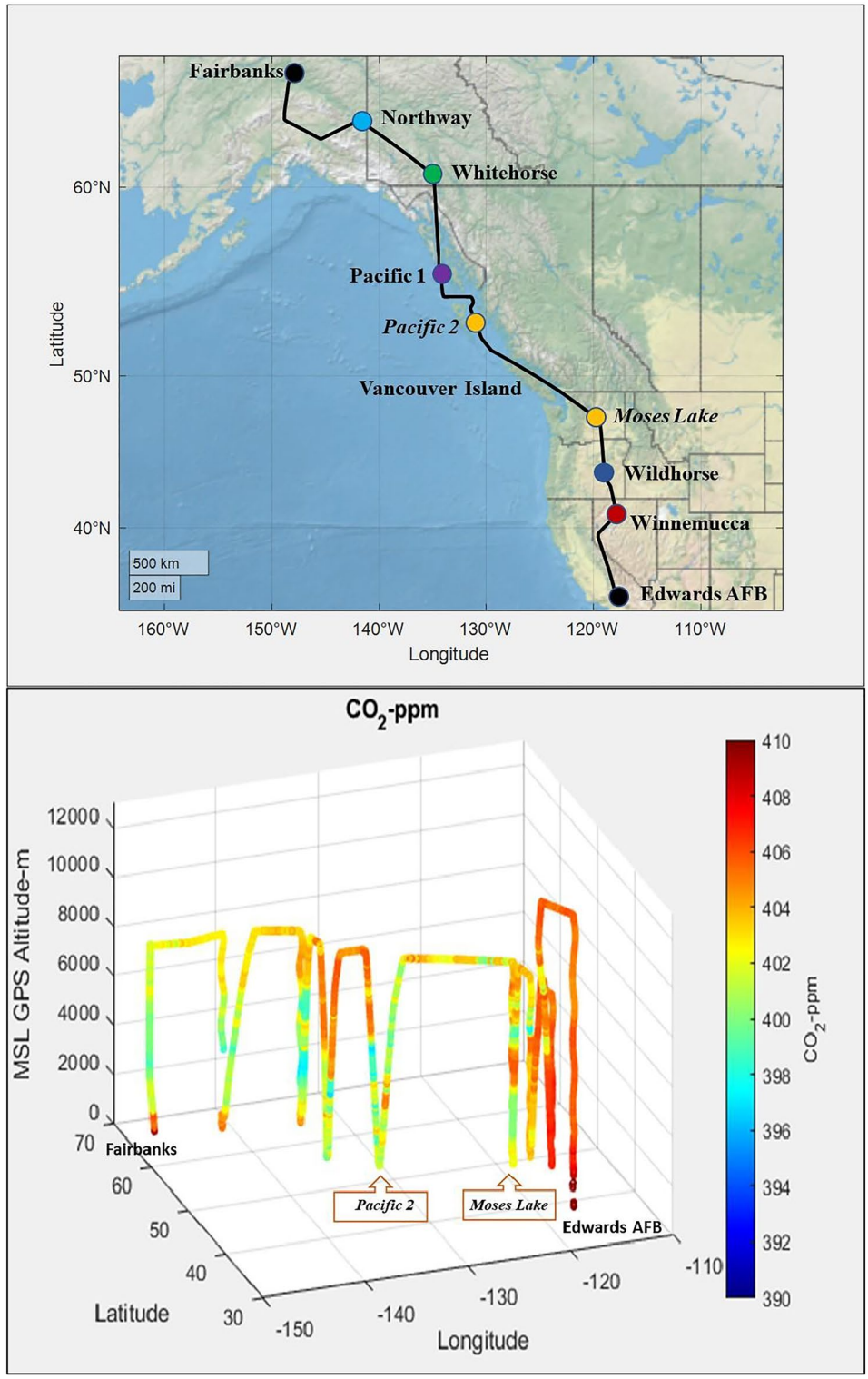


**Figure 1.** Top: map of the ground track for the return flight from Fairbanks, AK to Palmdale, CA on August 8, 2017. Fairbanks and the locations of eight spiral down flight segments are marked in circles, including two in-line descent-ascent maneuvers over Pacific Ocean labeled as Pacific 1 & Pacific 2. Bottom: 3-D (latitude, longitude, and flight altitude) sideview of in situ $CO_2$ mixing ratio measurements from onboard AVOCET for this flight. The data were sampled at 1-s intervals.

in Washington, Wildhorse airport in Oregon, Winnemucca airport in Nevada, and Edwards Air Force Base in California. The flight also conducted two in-line descent-ascent maneuvers above the Pacific Ocean just off the southern tip of Alaska before flying to Vancouver Island. Other than the spirals, almost all the flight was at 8–9 km altitude, except for the final segment between Reno NV and Edwards CA, which was flown at 12 km to allow sampling upper tropospheric air.

The bottom panel of Figure 1 shows in situ $CO_2$ concentrations at aircraft altitudes measured by AVOCET for the flight. AVOCET has a stated precision of ±0.1 ppm (1- sigma) and accuracy of ±0.25 ppm (Halliday et al., 2019). It shows significant horizontal and vertical gradients of $CO_2$ at the aircraft altitude, which is a typical seasonal pattern in the area. The $CO_2$ concentrations were higher near the surface at Fairbanks, Northway, and Whitehorse airports during the morning time of the flight due to the overnight accumulation of respiration and local emissions. Meanwhile, the higher $CO_2$ over Winnemucca, NV and Edwards Air Force Base, CA were presumably due to regional emissions, as there is little surface uptake over the deserts. The in situ measurements show high $CO_2$ in the free troposphere during the flight segment over Pacific Ocean and lower $CO_2$ in the following segment onto land before the spiral at Moses Lake, WA. It was notable that no outstanding $CO_2$ enhancements were seen at the aircraft altitude between the spirals at Pacific 2 and Moses Lake compared to $CO_2$ values at the same flight altitude before and after the segment.

### 2.2. $XCO_2$ Measurements From the $CO_2$ Sounder Lidar

The airborne $CO_2$ Sounder lidar uses a tunable laser to measure absorption across the vibration–rotational line of $CO_2$ centered at 1572.335 nm (Abshire et al., 2018). The lidar transmits 1-μs wide laser pulses at a rate of 10 kHz and the laser is stepped in 30 wavelengths across the $CO_2$ line at a rate of 300 Hz. The wavelength separation of each laser pulse was 250 MHz near line center and increased to 2 GHz at line wings to allow for more online samples. The laser line width is narrower than 30 MHz. The spectral resolution of the laser is over two hundred times higher than that of GOSAT, over three hundred times higher than that of OCO-2, and over 20 times higher than that of the ground-based Fourier Transform Spectrometers for the Total Carbon Column Observing Network (Wunch et al., 2011). The high spectral resolution allows sampling the fully resolved $CO_2$ line shape, including line width and line center position (Ramanathan et al., 2013), resulting in high sensitivity to $CO_2$ changes in the atmospheric column (Mao & Kawa, 2004).

The lidar retrieval algorithm uses a least-squares fit between the 30 wavelengths of the lidar measurements and the calculated $CO_2$ absorption line shape to retrieve $XCO_2$ (Ramanathan et al., 2018; Sun et al., 2021). The approach allows use of a standard linear least squares method to simultaneously solve for Doppler frequency shift, surface reflectance at off-line wavelengths, and a linear non-uniformity (slope) in the receiver spectral response as well.

In the retrieval forward calculations, the spectroscopy database HITRAN 2008 (Rothman et al., 2009) and the Line-By-Line Radiative Transfer Model (Clough et al., 1992; Clough & Iacono, 1995) V12.1 were used to calculate $CO_2$ optical depth and create look-up tables (LUTs) for a prior with a vertically uniform $CO_2$ concentration of 400 ppm. We then used these LUTs to retrieve the best-fit $XCO_2$ by comparing the lidar sampled line shapes with the calculated absorption line shapes and then scaling the prior without any inversion constraints. The retrievals used the atmosphere state (pressure, temperature, and water vapor profiles) from the near real time forward processing data of the Goddard Earth Observing System Model, Version 5 (GEOS-5; Rienecker et al., 2011). Data on the full model grid (0.25° latitude × 0.3125° longitude × 72 vertical layers, every 3h) were interpolated to flight ground track position and time for the atmospheric $CO_2$ and $H_2O$ absorption calculations.

## 3. Data Analysis Results

### 3.1. $CO_2$ Enhancements From BC Wildfires

Figure 2a shows the cloud-free $XCO_2$ retrievals from the lidar for the entire flight on August 8, 2017. Significant $XCO_2$ enhancements were clearly seen in the segment over Vancouver Island and across the Strait of Juan de Fuca into Washington State. Such $CO_2$ enhancements were not evident in the in situ measurements

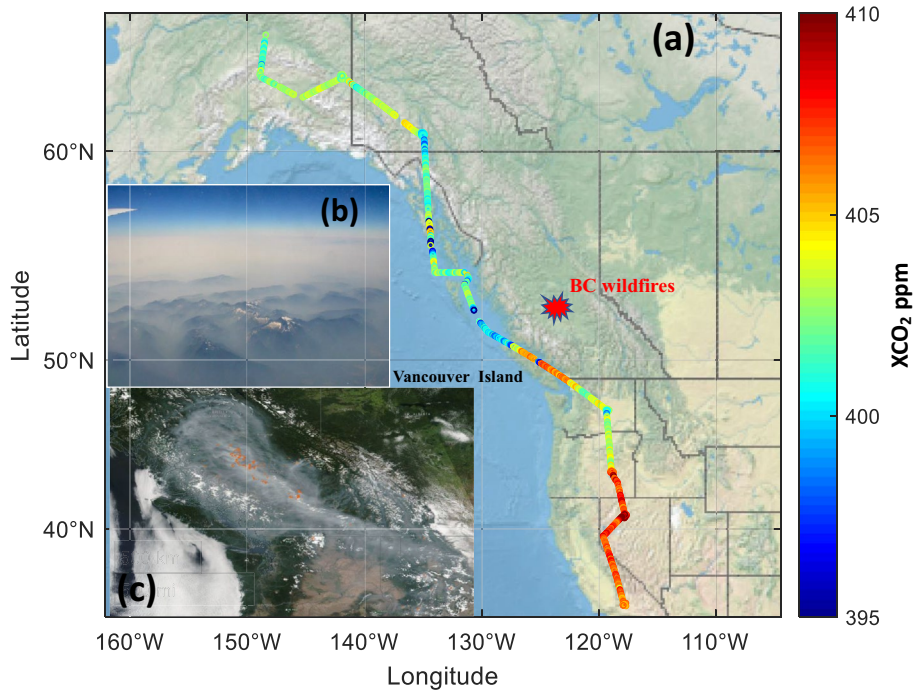


**Figure 2.** (a) The cloud-free $XCO_2$ retrievals from the $CO_2$ Sounder lidar for the flight on August 8, 2017. Significant $XCO_2$ enhancements were seen in the flight segment crossing Vancouver Island. The British Columbia wildfires are marked to the north of these enhancements. (b) Image of the smoke plumes from the wildfires in Canadian Rockies as seen from DC-8 over Vancouver Island (Photo by Graham Allan). (c) True color image from Aqua/MODIS showing the smoke and fires on the same day.

at flight altitudes (Figure 1). Compared to single-point in situ measurements, this shows a benefit of the lidar's $XCO_2$ measurements to capture $CO_2$ variations in the full atmospheric column below the aircraft.

The smoke plumes from wildfires in the Canadian Rockies were clearly seen from DC-8 aircraft over Vancouver Island and the fire and thermal anomalies map from Aqua/MODIS on the same day (Figures 2b and 2c). The smoke plumes were transported by wind from the Canadian Rockies into eastern Washington State and further down into Montana. Meanwhile, some smoke plumes and a large amount of $CO_2$ emissions from the fires were also transported to Vancouver Island.

Figure 3 shows the time series of the cloud-free $XCO_2$ retrievals together with the attenuated backscatter profiles for the flight segment from Pacific Ocean to Washington State. Dense smoke layers were seen in the lidar backscatter profiles near Vancouver Island and peaked at the top of the boundary layer near 2 km. The lidar range was used to distinguish ground returns from cloud returns after comparison to onboard radar altimetry. The $XCO_2$ retrievals over Vancouver Island and western Washington State have a median value of 406.5 ppm. The $XCO_2$ computed from the in situ vertical profiles of $CO_2$ mixing ratio during the spiral maneuvers at Pacific 2 and Moses Lake were 401.9 and 402.6 ppm, respectively. Therefore, the averaged $XCO_2$ enhancement within the segment from Vancouver Island to western Washington State was estimated to be 4 ppm. The $XCO_2$ enhancement segment spanned about 30 min, which at DC-8 aircraft speed of 200 m/s, corresponds to a ground-track length of 360 km.

### 3.2. Validation of the Lidar $XCO_2$ Measurements

A vertical spiral-down maneuver was conducted shortly after the $CO_2$ enhancement segment shown in Figure 3 from a flight altitude of 9 km to ground over Moses Lake in central Washington State. This allowed a comparison between the $XCO_2$ retrievals from the lidar and those constructed from the in situ vertical profile of $CO_2$. During the spiral hazy conditions were seen below 4.5 km in the lidar backscatter profiles (Figure 3). The AVOCET analyzer sampled every 1-s and the lidar $XCO_2$ retrievals were also based on 1-s

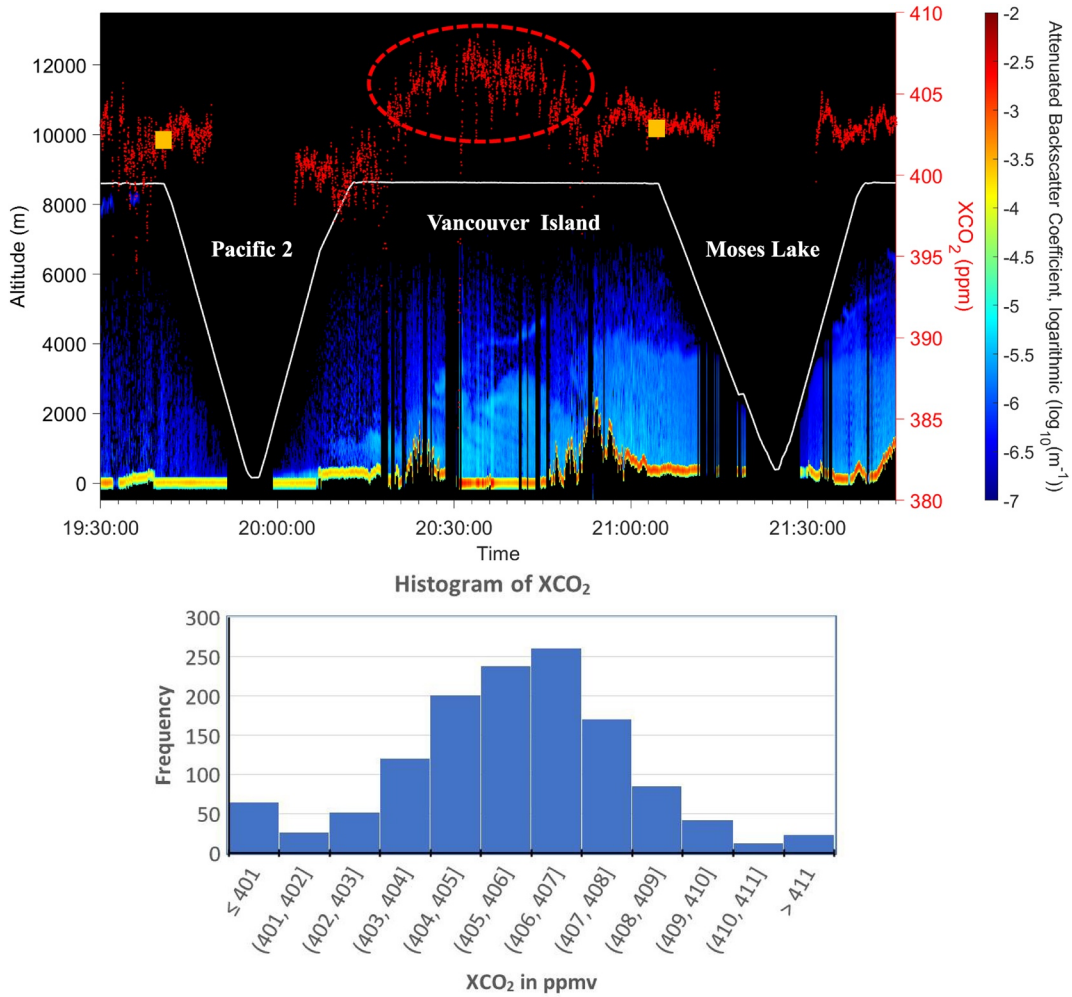


**Figure 3.** Top: the time series of cloud-free $XCO_2$ retrievals from the 1-s averaged lidar data (right axis) and the range-corrected attenuated backscatter profiles sampled at a vertical resolution of 15-m. Ground returns are strong and colored in yellow and red, and the returns from aerosols are light blue. The red dots are the 1-s $XCO_2$ retrievals smoothed with 9-point running mean. Aircraft GPS flight altitudes are marked in a white line. For reference, orange squares are the in situ $XCO_2$ from AVOCET during the second in-line descent-ascent maneuver over Pacific Ocean and the spiral down maneuver at Moses Lake airport, Washington. The $XCO_2$ enhancements near Vancouver Island are circled. Bottom: a histogram of the 1-s averaged $XCO_2$ retrievals in the enhancement segment.

averaged laser signals returned from ground. For the best estimation of the atmosphere state during the spiral maneuver, these retrievals used vertical profiles simultaneously measured by onboard DC-8 in situ instruments at an interval of 1-s. The in situ $XCO_2$ was computed from the in situ vertical profile integrated using the lidar's retrieval averaging kernel as vertical weighting. Both lidar and in situ $XCO_2$ were then averaged in each 1-km atmosphere layer for comparison. Figure 4 shows an average difference of less than 0.1 ppm for flight altitudes above 5-km and an average standard deviation of approximately 1 ppm. Validation results from other profiles throughout the campaign were within ±0.5 ppm (1-sigma) of the in situ data. Therefore, the 4 ppm $XCO_2$ enhancement from the Canadian wildfires was highly significant in relative to the lidar measurement uncertainty.

### 3.3. Improving Estimates of $CO_2$ Emissions From Wildfires

Figure 5 shows the integrated $XCO_2$ below 320 mb (~9 km) from $CO_2$ simulations by the Goddard PCTM (Kawa et al., 2004, 2010) on the same day. Note that averaging kernels were not applied to the model $XCO_2$ for estimating relative changes due to fire emissions. The PCTM $CO_2$ simulation is driven by meteorological

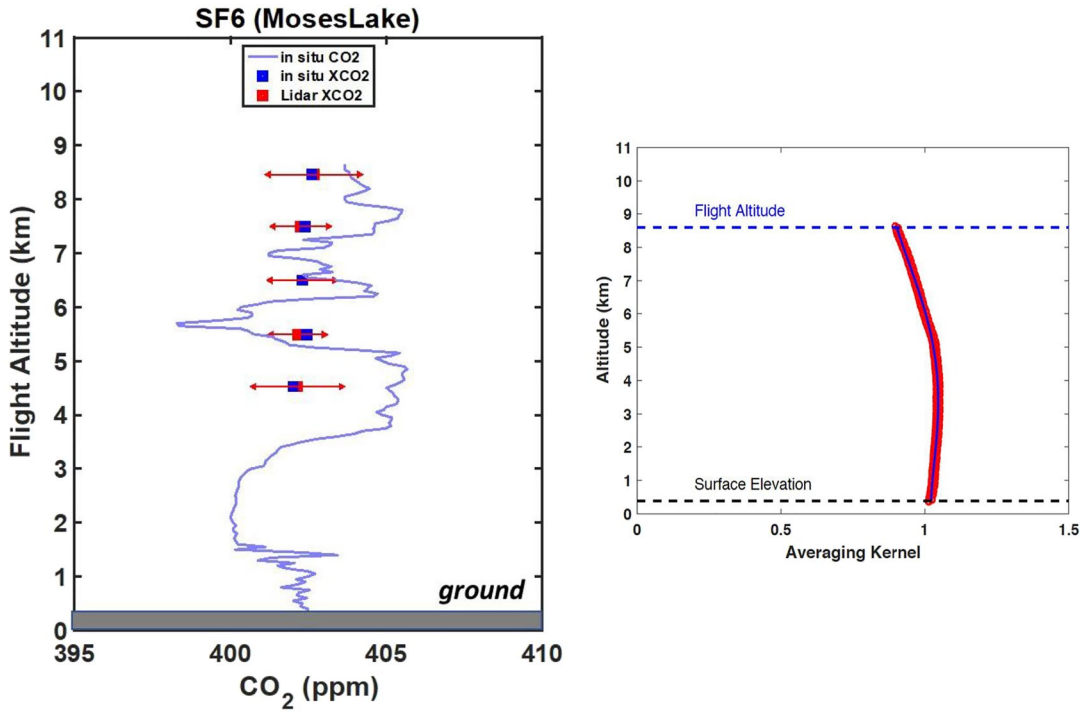


**Figure 4.** Comparison of cloud-free lidar $XCO_2$ retrievals with those from in situ measurements as a function of flight altitude during the spiral maneuver at Moses Lake, WA on August 8, 2017. The in situ $XCO_2$ values are marked in blue squares and the lidar's $XCO_2$ retrieval values are marked in red squares. The red error bars are ±1 standard deviation of the lidar's $XCO_2$ retrievals. The $XCO_2$ vertical averaging kernel for this profile segment is shown at right.

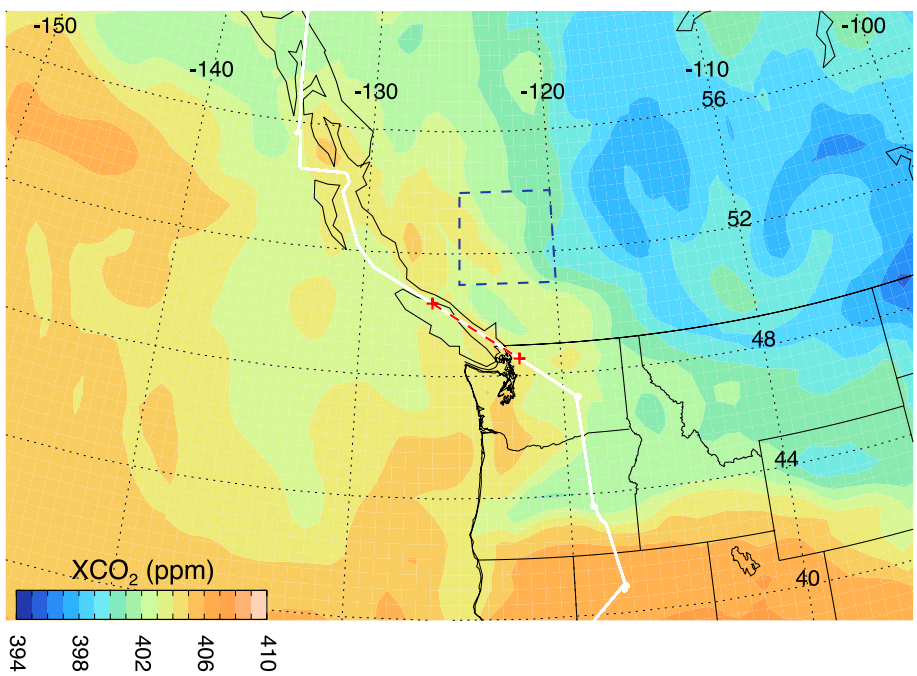


**Figure 5.** Map of $XCO_2$ (ppm) from ground to 320 mb simulated by Goddard Parameterized Chemistry Transport Model at 21 GMT on August 8, 2017. White line is the ground track of the airborne campaign flight and the two red pluses and red dashed line mark the flight segment where the $XCO_2$ enhancements were seen in the lidar retrievals. The box delineated by the dashed blue line indicates the area over which the British Columbia fire emissions were calculated.

data from the Modern-Era Retrospective analysis for Research and Applications (Bosilovich, 2013), which is a NASA reanalysis using GEOS-5. The vertical mixing in PCTM is parameterized for both turbulent diffusion in the boundary layer and convection. PCTM is run at 0.625° longitude × 0.5° latitude with 56 hybrid vertical levels and outputs hourly. PCTM uses GFED4s (including small fires) for the $CO_2$ emissions from wildfires. GFED includes an ecosystem model that uses satellite observations of burned area and ecosystem productivity to estimate fuel loads and combustion (van der Werf et al., 2017).

The modeled $XCO_2$ at 21 GMT shows enhancements up to ~2 ppm over the Canadian Rockies in response to a total release of 837 Gg C $day^{-1}$ from the BC fires within the area (51–54°N, 120–125°W) on August 8 estimated by GFED. The modeled $XCO_2$ enhancements near Vancouver Island (estimated from the local maximum on the contour map near the flight track in Figure 5 as well as from the model-interpolated $XCO_2$ along the track similar to Figure 3) were about 1 ppm. Compared to 4 ppm averaged enhancement of lidar $XCO_2$ for the equivalent atmospheric columns, the modeled enhancements were low. The underestimate of $XCO_2$ in the model could be due in part to model diffusion and transport shortcomings. Given, however, the spatial scale of the observed $XCO_2$ perturbation (~360 km) and multi-day duration of the fires, along with past performance of PCTM using analyzed winds to simulate $CO_2$ gradients in frontal systems and other relatively fine-scale features (Parazoo et al., 2008) as well as the parent GEOS-5 model use for aerosol plume simulations, we expect that the $XCO_2$ perturbation would be close to that observed if the emissions were correct. The daily $CO_2$ release estimate from another data set of fire emissions, the Quick Fire Emissions Dataset (QFED; Darmenov & da Silva, 2015), in the same area on the same day was 1,122 Gg C $day^{-1}$. The QFED estimate was 34% higher than that from GFED but proportionally still underestimated at least by a factor of 2. QFED is based on the detection of fire radiative power calibrated against observations of aerosol optical depth. Our findings in this case study highlight the potential of airborne and spaceborne lidar $XCO_2$ measurements for evaluating atmospheric models and global emissions inventories.

## 4. Conclusion and Discussion

Analysis of lidar measurements from the summer 2017 ASCENDS/ABoVE airborne science campaign show the capability to measure $XCO_2$ enhancements through dense smoke plumes from wildfires in British Columbia, Canada. On the overpass of Vancouver Island on August 8, the retrievals from the lidar measurements showed an average 4 ppm enhancement in $XCO_2$ beneath the aircraft. A spiral maneuver made after the smoke plume showed the $XCO_2$ measurements had small bias and high precision, and a high spatial resolution (~200-m). The modeled enhancements from the Goddard PCTM which uses the GFED fire emission database were about 1 ppm near Vancouver Island. The result suggests that the $CO_2$ emissions from GFED for the BC wildfires were underestimated by a factor of two or more for that day.

The results show that future airborne campaigns and spaceborne missions with this capability should improve modeling of $CO_2$ emissions from wildfires. This will benefit atmospheric transport process studies, carbon data assimilation, and global and regional carbon flux estimates. Along with the expected increase in the net contribution of forest fires to global carbon emissions, improved capabilities to constrain wildfire emissions is greatly needed.

**Acknowledgments**
This work was supported by the NASA ASCENDS pre-formulation activity, the ABoVE project, and the Airborne Science Program. We gratefully acknowledge the work of the DC-8 team at NASA Armstrong Flight Center for helping plan and conduct the flight campaign. We also thank Joshua P. DiGangi, Glenn Diskin and Yonghoon Choi from NASA Langley Research Center for providing the in situ $CO_2$ and $H_2O$ data. This paper is dedicated to our friend and colleague Dr. Graham R. Allan who had a key role in the 2017 ASCENDS/ABoVE airborne campaign but who passed away in May 2020. Dr. Allan's work was essential in the development of the Goddard $CO_2$ Sounder lidar, airborne campaigns, and data analysis over the past decade and he is missed. We thank two anonymous reviewers whose edits and comments/suggestions helped improve and clarify this manuscript.

## Data Availability Statement

All the data used in this work can be downloaded at the LaRC airborne science data site, https://www-air.larc.nasa.gov/cgi-bin/ArcView/ascends.2017.

## References

Aben, I., Hasekamp, O., & Hartmann, W. (2007). Uncertainties in the space-based measurements Of $CO_2$ columns due to scattering in the Earth's atmosphere. *Journal of Quantitative Spectroscopy & Radiative Transfer*, *104*, 450–459. https://doi.org/10.1016/j.jqsrt.2006.09.013

Abshire, J. B., Ramanathan, A., Riris, H., Mao, J., Allan, G. R., Hasselbrack, W. E., et al. (2014). Airborne measurements of $CO_2$ column concentration and range using a pulsed direct-detection IPDA lidar. *Optical Remote Sensing of the Atmosphere*, *6*(1), 443–469. https://doi.org/10.3390/rs6010443

Abshire, J. B., Ramanathan, A. K., Riris, H., Allan, G. R., Sun, X., Hasselbrack, W. E., et al. (2018). Airborne measurements of $CO_2$ column concentrations made with a pulsed IPDA lidar using a multiple-wavelength-locked laser and HgCdTe APD detector. *Atmospheric Measurement Techniques*, *11*, 2001–2025. https://doi.org/10.5194/amt-11-2001-2018

Abshire, J. B., Riris, H., Allan, G. R., Weaver, C. J., Mao, J., Sun, X., et al. (2010). Pulsed airborne lidar measurements of atmospheric $CO_2$ column absorption. *Tellus*, *62*, 770–783. https://doi.org/10.1111/j.1600-0889.2010.00502.x

Abshire, J. B., Riris, H., Weaver, C. W., Mao, J., Allan, G. R., Hasselbrack, W. E., et al. (2013). Airborne measurements of $CO_2$ column absorption and range using a pulsed direct-detection integrated path differential absorption lidar. *Applied Optics*, *52*, 4446–4461. https://doi.org/10.1364/ao.52.004446

Andela, N., Morton, D. C., Giglio, L., Chen, Y., van der Werf, G. R., Kasibhatla, P. S., et al. (2017). A human-driven decline in global burned area. *Science (New York, N.Y.)*, *356*(6345), 1356–1362. https://doi.org/10.1126/science.aal4108

Andreae, M. O. (2019). Emission of trace gases and aerosols from biomass burning – An updated assessment. *Atmospheric Chemistry and Physics*, *19*, 8523–8546. https://doi.org/10.5194/acp-19-8523-2019

Bosilovich, M. G. (2013). Regional climate and variability of NASA MERRA and recent reanalyses: U.S. summertime precipitation and temperature. *Journal of Applied Meteorology &Climatology*, *52*, 1939–1951. https://doi.org/10.1175/JAMC-D-12-0291

Butz, A., Hasekamp, O. P., Frankenberg, C., & Aben, I. (2009). Retrievals of atmospheric $CO_2$ from simulated space-borne measurements of backscattered near-infrared sunlight: Accounting for aerosol effects. *Applied Optics*, *48*, 3322–3336. https://doi.org/10.1364/ao.48.003322

Ciais, P., Sabine, C., Bala, G., Bopp, L., Brovkin, V., Canadell, J., et al. (2013). Carbon and Other Biogeochemical Cycles, chap. 6. In T. F. Stocker, D. Qin, G.-K. Plattner, M. Tignor, S. K. Allen, J. Boschung, A. Nauels, Y. Xia, V. Bex, & P. M. Midgley (Eds.), *IPCC, climate change 2013: The physical science basis. Contribution of working group I to the fifth assessment report of the intergovernmental panel on climate Change* (Vol. 465–570). Cambridge University Press.

Clough, S. A., & Iacono, M. J. (1995). Line-by-line calculation of atmospheric fluxes and cooling rates 2. Application to carbon dioxide, methane, nitrous oxide and the halocarbons. *Journal of Geophysical Research*, *100*, 16519–16535. https://doi.org/10.1029/95JD01386

Clough, S. A., Iacono, M. J., & Moncet, J. (1992). Line-by-line calculations of atmospheric fluxes and cooling rates: Application to water vapor. *Journal of Geophysical Research*, *97*, 15761–15785. https://doi.org/10.1029/92JD01419

Crisp, D., Atlas, R. M., Breon, F.-M., Brown, L. R., Burrows, J. P., Ciais, P., et al. (2004). The Orbiting Carbon Observatory (OCO) mission. *Advances in Space Research*, *34*(4), 700–709. https://doi.org/10.1016/j.asr.2003.08.062

Darmenov, A., & da Silva, A. (2015). *The Quick Fire Emissions Dataset (QFED): Documentation of versions 2.1, 2.2 and 2.4*, NASA Technical Report Series on Global Modeling and Data Assimilation NASA TM-2015-104606 (Vol. 38). http://gmao.gsfc.nasa.gov/pubs/docs/Darmenov796.pdf

Diskin, G. S., Podolske, J. R., Sachse, G. W., & Slate, T. A. (2002). Open-path airborne tunable diode laser hygrometer. Proc. SPIEDiode Lasers and Applications in Atmospheric Sensing. https://doi.org/10.1117/12.453736

Duran, B. C. year in review(2017). Wildfires devastate the province like never before. https://globalnews.ca/news/3921710/b-c-year-in-review-2017-wildfires/2017

Guerlet, S., Butz, A., Schepers, D., Basu, S., Hasekamp, O. P., Kuze, A., et al. (2013). Impact of aerosol and thin cirrus on retrieving and validating $XCO_2$ from GOSAT shortwave infrared measurements. *Journal of Geophysical Research: Earth and Space Science*, *118*, 4887–4905. https://doi.org/10.1002/jgrd.50332

Halliday, H. S., DiGangi, J. P., Choi, Y., Diskin, G. S., Pusede, S. E., Rana, M., et al. (2019). Using short-term CO/CO 2 ratios to assess air mass differences over the Korean Peninsula during KORUS-AQ. *Journal of Geophysical Research: Atmospheres*, *124*(20), 10951–10972. https://doi.org/10.1029/2018JD029697

Houweling, S., Hartmann, W., Aben, I., Schrijver, H., Skidmore, J., Roelofs, G.-J., & Breon, F.-M. (2005). Evidence of systematic errors in SCIAMACHY-observed $CO_2$ due to aerosols. *Atmospheric Chemistry and Physics*, *5*, 3003–3013. https://doi.org/10.5194/acp-5-3003-2005

Kawa, S. R., Abshire, J. B., Baker, D. F., Browell, E. V., Crisp, D., Crowell, S. M. R., et al. (2018). Active Sensing of CO2 Emissions over Nights, Days, and Seasons (ASCENDS): Final Report of the ASCENDS Ad Hoc Science Definition Team, Document ID: 20190000855. NASA/TP–2018-219034. GSFC-E-DAA-TN64573.

Kawa, S. R., Erickson, D. J., III, Pawson, S., & Zhu, Z. (2004). Global $CO_2$ transport simulations using meteorological data from the NASA data assimilation system. *Journal of Geophysical Research*, *109*, D18312. https://doi.org/10.1029/2004JD004554

Kawa, S. R., Mao, J., Abshire, J. B., Collatz, G. J., Sun, X., & Weaver, C. J. (2010). Simulation studies for a space-based $CO_2$ lidar mission. *Tellus B: Chemical and Physical Meteorology*, *62*, 770–783. https://doi.org/10.1111/j.1600-0889.2010.00486.x

Kuze, A., Suto, H., Shiomi, K., Kawakami, S., Tanaka, M., Ueda, Y., et al. (2016). Update on GOSAT TANSO-FTS performance, operations, and data products after more than 6 years in space. *Atmospheric Measurement Techniques*, *9*, 2445–2461. https://doi.org/10.5194/amt-9-2445-2016

Le Quéré, C., Andrew, R. M., Friedlingstein, P., Sitch, S., Hauck, J., Pongratz, J., et al. (2018). Global carbon budget 2018. *Earth System Science Data*, *10*, 2141–2194. https://doi.org/10.5194/essd-10-2141-2018

Lombrana, L. M., Warren, H., & Rathi, A. (2020). *Measuring the Carbon-dioxide cost of last year's worldwide wildfires*. https://www.bloomberg.com/graphics/2020-fire-emissions/

Mao, J., Abshire, J. B., Kawa, S. R., Riris, H., Allan, G. R., Hasselbrack, W. E., et al. (2019). *$CO_2$ laser Sounder lidar: Toward atmospheric CO2 measurements with high-precision, Low-bias and global coverage. A43D-01 presented at the Fall Meeting* (pp. 9–13). AGU.

Mao, J., & Kawa, S. R. (2004). Sensitivity studies for space-based measurement of atmospheric total column carbon dioxide by reflected sunlight. *Applied Optics*, *43*, 914–927. https://doi.org/10.1364/ao.43.000914

Mao, J., Ramanathan, A., Abshire, J. B., Kawa, S. R., Riris, H., Allan, G. R., et al. (2018). Atmospheric $CO_2$ concentration measurements to cloud tops from airborne lidar measurement during ASCENDS science campaigns. *Atmospheric Measurement Techniques*, *11*, 127–140. https://doi.org/10.5194/amt-11-127-2018

Meyer, C. P., Cook, G. D., Reisen, F., Smith, T. E. L., Tattaris, M., Russell-Smith, J., et al. (2012). Direct measurements of the seasonality of emission factors from savanna fires in northern Australia. *Journal of Geophysical Research*, *117*, D20305. https://doi.org/10.1029/2012JD017671

Obland, M. D., Corbett, A. M., Lin, B., Meadows, B., Campbell, J. F., Kooi, S., et al. (2018). Advancements towards active remote sensing of $CO_2$ from space using intensity-modulated, continuous-Wave (IM-CW) lidar, Proc. SPIE 10785, Sensors, Systems, and Next-Generation Satellites XXII, 1078509. https://doi.org/10.1117/12.2325816

Parazoo, N., Denning, A. S., Kawa, S. R., Corbin, K., Lokupitia, R., Baker, I., & Worthy, D. (2008). Mechanisms for synoptic transport of $CO_2$ in the midlatitudes and tropics. *Atmospheric Chemistry and Physics*, *8*, 7239–7254. https://doi.org/10.5194/acp-8-7239-2008

Ramanathan, A. K., Mao, J., Abshire, J., & Allan, G. R. (2015). Remote sensing measurements of the $CO_2$ mixing ratio in the planetary boundary layer using cloud slicing with airborne lidar. *Geophysical Research Letters*, *42*, 2055–2062. https://doi.org/10.1002/2014gl062749

Ramanathan, A. K., Mao, J., Allan, G. R., Riris, H., Weaver, C. J., Hasselbrack, W. E., et al. (2013). Spectroscopic measurements of a $CO_2$ absorption line in an open vertical path using an airborne lidar. *Applied Physics Letters*, *103*, 214102. https://doi.org/10.1063/1.4832616

Ramanathan, A. K., Nguyen, H. M., Sun, X., Mao, J., Abshire, J. B., Hobbs, J. M., & Braverman, A. J. (2018). A singular value decomposition framework for bias-free retrievals with vertical distribution information from column greenhouse gas absorption spectroscopy measurements. *Atmospheric Measurement Techniques*, *11*, 4909–4928. https://doi.org/10.5194/amt-11-4909-2018

Rienecker, M. M., Suarez, M. J., Gelaro, R., Todling, R., Bacmeister, J., Liu, E., et al. (2011). MERRA: NASA's modern-era retrospective analysis for research and applications. *Journal of Climate*, *24*, 3624–3648. https://doi.org/10.1175/jcli-d-11-00015.1

Rothman, L., Gordon, I. E., Barbe, A., Chris Benner, D., Bernath, P. F., Birk, M., et al. (2009). The HITRAN 2008 molecular spectroscopic database. *Journal of Quantitative Spectroscopy & Radiative Transfer*, *110*(9), 533–572. https://doi.org/10.1016/j.jqsrt.2009.02.013

Sun, X., Abshire, J. B., Ramanathan, A., Kawa, S. R., & Mao, J. (2021). Retrieval algorithm for the column $CO_2$ mixing ratio from pulsed multi-wavelength lidar measurements. *Atmospheric Measurement Techniques*, *14*, 3909–3922. https://doi.org/10.5194/amt-14-3909-2021

Tian, H., Lu, C., Ciais, P., Michalak, A. M., Canadell, J. G., Saikawa, E., et al. (2016). The terrestrial biosphere as a net source of greenhouse gases to the atmosphere. *Nature*, *531*, 225–228. https://doi.org/10.1038/nature16946

Torres, O., Bhartia, P. K., Taha, G., Jethva, H., Das, S., Colarco, P., et al. (2020). Stratospheric injection of massive smoke plume from Canadian boreal fires in 2017 as seen by DSCOVR-EPIC, CALIOP, and OMPS-LP observations. *Journal of Geophysical Research: Atmospheres*, *125*, e2020JD032579. https://doi.org/10.1029/2020JD032579

Uchino, O., Kikuchi, N., Sakai, T., Morino, I., Yoshida, Y., Nagai, T., et al. (2012). Influence of aerosols and thin cirrus clouds on the GOSAT-observed $CO_2$: A case study over Tsukuba. *Atmospheric Chemistry and Physics*, *12*, 3393–3404. https://doi.org/10.5194/acp-12-3393-2012

van der Werf, G. R., Randerson, J. T., Giglio, L., van Leeuwen, T. T., Chen, Y., Rogers, B. M., et al. (2017). Global fire emissions estimates during 1997–2016. *Earth System Science Data*, *9*, 697–720. https://doi.org/10.5194/essd-9-697-2017

Wunch, D., Toon, G. C., Blavier, J.-F. L., Washenfelder, R. A., Notholt, J., Connor, B. J., et al. (2011). The total carbon column observing network. *Philosophical Transactions of the Royal Society A*, *369*, 2087–2112. https://doi.org/10.1098/rsta.2010.0240